Lawrence Berkeley National Laboratory

Title
Possible Diamond-Like Nanoscale Structures Induced by Slow Highly-Charged Ions on Graphite (HOPG)

Permalink
https://escholarship.org/uc/item/27v431df

Author
Sideras-Haddad, E.

Publication Date
2009-10-13

Accepted Manuscript

Possible Diamond-Like Nanoscale Structures Induced by Slow Highly-Charged Ions on Graphite (HOPG)
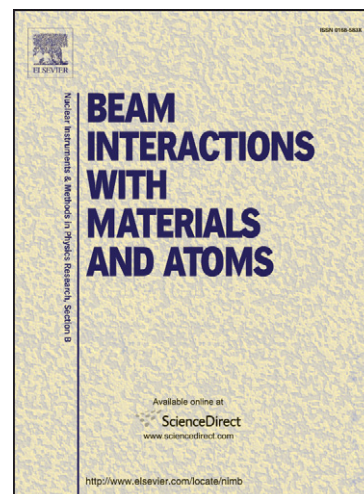
E. Sideras-Haddad, T. Schenkel, S. Shrivastava, T. Makgato, A. Batra, C.D. Weis, A. Persaud, R. Erasmus, B. Mwakikunga

Possible Diamond-Like Nanoscale Structures Induced by Slow Highly-Charged Ions on Graphite (HOPG)

E. Sideras-Haddad[a,c], T. Schenkel[b], S. Shrivastava[a], T. Makgato[a], A. Batra[b], C. D. Weis[b], A. Persaud[b]
R. Erasmus[a] and B. Mwakikunga[a]

[a] School of Physics, University of the Witwatersrand, Wits 2050, Johannesburg, South Africa.
[b] E. O. Lawrence Berkeley National Laboratory, Berkeley, CA 94720
[c] iThemba LABS for Accelerator Based Sciences, Johannesburg-Gauteng, South Africa

Abstract

The interaction between slow highly-charged ions (SHCI) of different charge states from an electron-beam ion trap and highly-oriented pyrolytic graphite (HOPG) surfaces is studied in terms of modification of electronic states at single-ion impact nanosize areas. Results are presented from AFM/STM analysis of the induced-surface topological features combined with Raman spectroscopy. I–V characteristics for a number of different impact regions were measured with STM and the results argue for possible formation of diamond-like nanoscale structures at the impact sites.

I. Introduction

The fabrication of surface nanostructures is of paramount importance in the constantly developing areas of nanotechnology. It is only recently that the unique qualities of slow highly-charged ions are being appreciated and make these ions an exceptional

means for studying nanostructuring surfaces[1,2]. One of the unique features that characterises slow highly-charged ions is their immense potential energy (the sum of the ionization potentials) and slow kinetic energy (velocities are lower than the Bohr velocity, $v_{Bohr} = 2.19\text{x}10^6 \ ms^{-1}$) in contrast to singly-charged fast ions commonly used in implantation and ion/solid=interactions in general. Such attributes are mainly due to the deposition of large amounts of potential energy on the surface of the solid within a 10 fs time scale, the intense electronic excitation with equivalent power densities of the order of $\sim10^{14}\text{W/cm}^2$ [2, 3, 4], the highly spatial localisation of the excitation and the formation of nano-defects on the surface of the target material.

The manner in which the solid surface responds to the transfer of the large potential energy of the highly-charged ions defines in a sense the different possibilities in terms of applications. The later include highly-charged ion-based lithography and surface patterning, surface cleaning or "soft sputtering" and structural and electronic surface

modifications. The initial recipient of the large potential energy of the incoming SHCI is the electronic system of the surface. Electron emission and sputtering yields are exceptionally high and increase strongly as a function of the potential energy of projectiles[5]. The neutralisation process of the SHCI is extremely fast, of the order of a few femtoseconds, during which a surface domain with high ionisation density is formed. As electrons from the surrounding solid cannot replace promptly the removed electrons, the impact area cannot be neutralised within time scales of less than several picoseconds, and the localised charged region can suffer a Coulomb explosion, forming in this manner surface defects at the nanoscale level[6, 7, 8]. Such nanometer-size defects ranging between 3nm to 50nm have been observed in the form of craters or blisters in materials such as silicon[9], mica[10], highly-oriented pyrolytic graphite[11], SiO_2 and Al_2O_3[12] using atomic-force microscopy (AFM) and scanning tunnelling microscopy (STM). The detailed elucidation of the response to the intense, ultra-fast electronic

excitation induced by slow, highly-charged ions is a subject of ongoing research[13].

Recently, Hamza *et al.*[14] reported on observations of excitonic features in the luminescence from HCI-induced surface nanostructures in Si after intense, ultrafast electronic excitation of the surface. In a similar note, modification of electronic states by Ar^{8+} impact on HOPG has been observed by Meguro *et al.*[15, 16]. A subsequent surface treatment, after the Ar^{8+} bombardment, with electrons injected from an STM tip provided a localised transition from sp^2 to sp^3 hybridisation in HOPG, resulting in the formation of nanoscale diamond-like structures (nanodiamond) observed using Raman spectroscopy. This transformation was also induced by He–Cd laser irradiation and the transition barrier seems to be very low.

Similar studies investigating the effects of HCI on HOPG have been performed by Aumayer *et al.*[17] using low charge states and by

Gilaspy *et al.*[18] and Tona *et al.*[19] using much higher charge states. However, in these studies the evolution of the nano-defects during annealing and the possible modification of the electronic states and in particular a hydrogen-catalysed sp^2 to sp^3 hybridisation was not of concern.

In the present work, we report on results from *ex situ* AFM/STM imaging analysis and Raman spectroscopy on nanostructures induced on a HOPG surface after irradiation with Sb^{8+}, Sb^{20+} and Sb^{22+} and Bi^{35+} ion beams, and after annealing treatment in a hydrogen atmosphere. This study is motivated by the interest in assessing the optimum parameters for the formation of diamond-like carbon structures on HOPG in terms of size and quality (sp^3/sp^2 ratio) with respect to ion charge used and annealing conditions. Such information might also be helpful to our interest in the possibility of forming optically active nanodiamonds in ordered arrays via a single-ion implantation scheme[20] to be used in basic

quantum-information processing with N-V defect centres[21] in a nanodiamond matrix.

II. Experimental setup

Highly-charged ions were extracted from the Electron Beam Ion Trap (EBIT) at Lawrence Berkeley National Laboratory[22], and reached the target chamber after momentum analysis in a 90° bending magnet. The pressure in the target chamber was in the low 10^{-8} torr range. We emphasise that this study focuses on the applied aspects of defect formation under modest vacuum conditions as they are present in typical ion implanters, and not on atomically clean surfaces prepared under ultra-high vacuum conditions. Ion kinetic energies, $E_{kin} = q \times U_{ext}$, were set by the EBIT extraction potential $U_{ext} = 5$ kV and were 40 KeV, 90 KeV, 110 KeV and 175 KeV for the Sb^{8+}, Sb^{20+}, Sb^{22+} and Bi^{35+}

accordingly. Ions impinged on target under normal incidence. Typical ion currents were of the order of 4, 3, 11 and 5 one particle pA for the 8^+, 20^+, 22^+ and 35^+ charge states accordingly ($\sim 10^6$ ions/s) and total fluences were of the order of 100 ions per μm^{-2}.

The HOPG samples were cleaved by adhesive conducting tape in order to expose atomically flat terraces necessary for the subsequent AFM/STM analysis.

After SHCI irradiation the samples were transferred in air to an AFM for imaging of the impact sites. They were then transported to an annealing furnace and annealed in a hydrogen atmosphere at 650 °C for 40 min. Subsequent imaging analysis and conductivity measurements were performed using AFM and STM after annealing. The analysis of the defects was complemented by micro-Raman spectroscopy in order to assess the implantation damage before and after annealing and to characterise the nature of the induced nanostructures.

Morphological studies of the surface nanostructures at the ion impact sites were carried out using a di-Dimension 3100 and a di-CPII Veeco AFM/STM instrument. AFM imaging was performed in non-contact mode while STM imaging was performed using a 5 μm scanner.

III. Results and discussion

Non-contact AFM analysis shows the formation of nanometre-sized surface structures embedded in HOPG upon single, highly-charged ion impacts. These nanostructures are formed for all types and charge states of ions used. A typical image of such nano-dots is shown in Fig. 1.
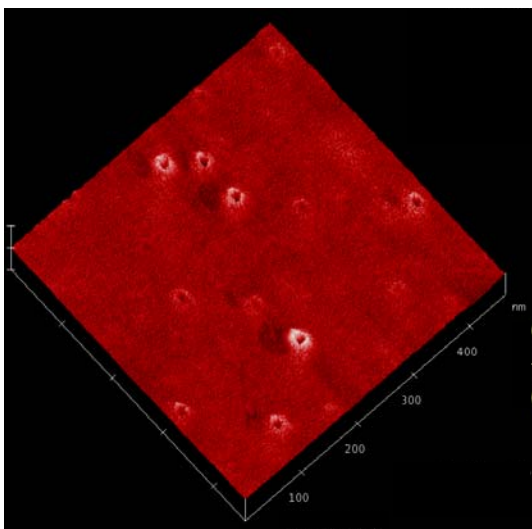
Figure1. Non-contact mode AFM image of nano-scale surface defects on HOPG bombarded with Sb 18+· ions.

The density of these nano-dots correlates well with the estimated ion fluence used during exposure of the order of 100 ions/μm^2. The area surrounding the nano-dot has remained unaffected by the impinging ions. A significant number of these nano-structures were inspected in terms of their physical size as a function of charge state used. As these nano-structures result from the large surface deposition of the potential energy that the ions carry rather

than their kinetic energy[17] the observed variation in size correlates well with the charge states used as shown in Fig. 2.
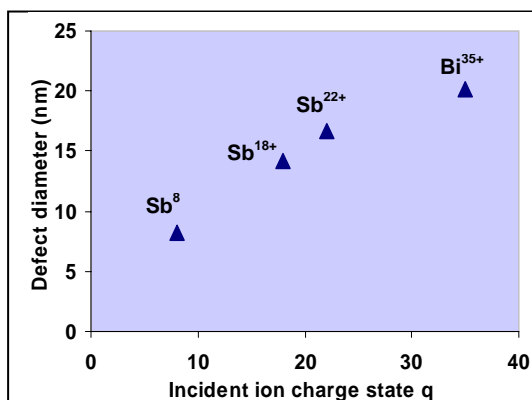

Figure 2. Size of surface nano-defect with respect to ion and charge state used.

First-order Raman analysis of the HOPG surface before annealing shows the 1580 cm^{-1} typical G-line. Normally one would expect to see also the 1354 cm^{-1} D-line due to lattice deformation and point defects due to the exposure. In previous studies by Tona *et al.*[23,24] the relation of the intensity ratio between the two Raman peaks and the potential energy of the projectile was established and used to assess the effect of charge states on the induced surface damage. In

the present investigation the ion fluence is few orders of magnitude less than the one used by Tona *et al*. The radiation damage therefore is small and non-observable by Raman spectroscopy. The Raman shift for diamond is 1331 cm^{-1}. This is very close to the Raman D-line. Given that the average fluence used during irradiations is of the order of 100 ions/μm^2 and taking into consideration the small size of the nanostructures observed, any electronic surface modification due to transitions from sp^2 to sp^3 hybridisation would generate a Raman signal that is very weak and will fall within the shoulder of the D-line, making it almost impossible to detect. This was the case even here where there was no contribution by the D-line due to the extremely low damage induced. The observation and characterisation of possible diamond-like nanostructures is therefore only achievable by careful AFM/STM analysis of the electronic properties of these nanostructures.

Fig. 3 shows a topological map of surface nano-defects taken with non-contact AFM of an exposed area to Sb^{18+} after annealing at 650 °C in hydrogen atmosphere.
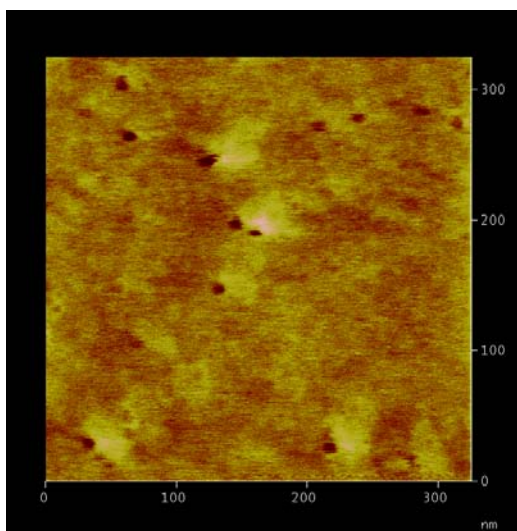

Figure 3. Typical non-contact AFM image of surface nano-defects induced by Sb^{18+} impact after annealing at 650 °C in hydrogen atmosphere.

I–V characteristics for a number of different impact regions exposed to all different types and charge states of ions used were measured by using scanning tunnelling microscopy (STM). Fig.4 shows an STM image of such nano-defects induced by Sb^{22+}.

After zooming into an impact region, I-V curves were obtained for several points around and across a few identified nanostructures. Fig. 5 shows a family of such I-V curves over a particular nanostructure induced by Sb^{22+}. In this manner, the evolution of the electronic properties across one particular nanostructure is mapped.
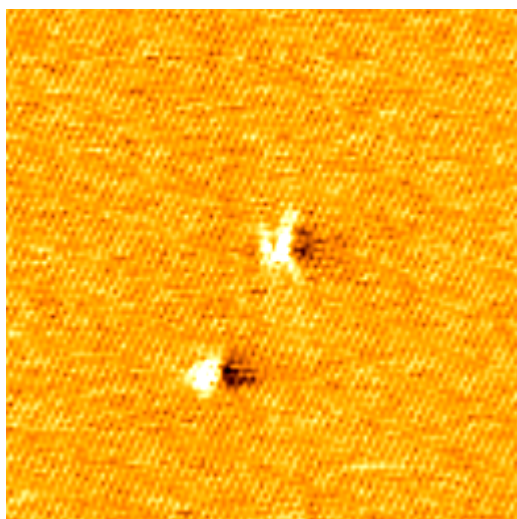

Figure 4. STM image of surface nanostructures induced in single-ion impacts using Sb^{22+}.

It is apparent that dramatic modification of the electronic states has taken place within the nanostructure area catalysed by hydrogen upon annealing. The I-V curves taken across the nano-dot seen in fig. 5 argue for a localised transition from sp^2 to sp^3 hybridisation in HOPG as seen also by Meguro *et al.* [15, 16, 25] working on a low charge state regime with Ar^{8+}. It has been argued by these authors that the large potential energy of slow Ar^{8+} induces strong localised electronic transitions resulting in modification of the electronic states of the impact area.

Subsequent surface treatment either by electron injection from an STM tip or by He–Cd laser irradiation provide a localised transition from sp^2 to sp^3 hybridisation in HOPG, resulting in the formation of nanoscale diamond-like structures (nanodiamond). Here the surface treatment was achieved by annealing the sample at 650 °C in a hydrogen atmosphere.
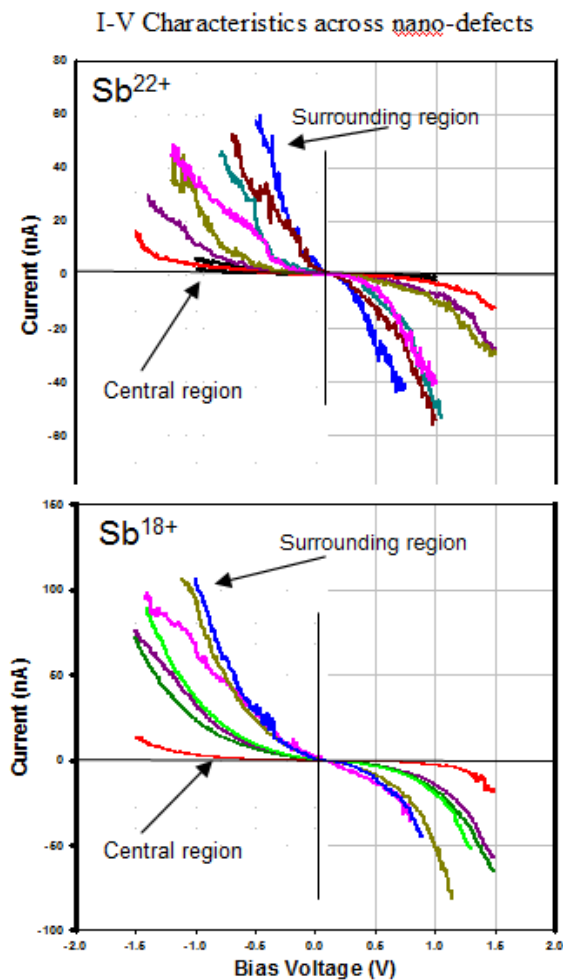
Figure 5. I-V characteristics measured with STM for various points across nano-defects and in the surrounding regions

It is well known that hydrogen plays a key role during any diamond synthetising process by catalysing the sp^2 to sp^3 hybridisation. Hydrogen radicals etch away any graphite forming

on a substrate, facilitating only diamond growth. Hydrogen terminates also the surface dangling carbon bonds, stabilising in this manner the surface and preventing it from reconstructing into other non-diamond allotropes.

IV. Conclusions

The interaction of highly-charged ions with charged states between 8^+ and 35^+ and HOPG surface results in the formation of nano-scale surface defects. The intense highly-localised electronic excitations result in modifications of the electronic states within nanometre areas. Further appropriate surface treatment seems to trigger a change from sp^2 to sp^3 hybridisation due to possible lowering of the potential barrier for such transformation by depleting electrons upon the highly-charged ion impacts[25].

With the recently developed single-ion implantation techniques[26, 20] it becomes possible to form ordered arrays of nanodiamond

(nanodiamond-like) structures which could be used in many interesting applications. We are particularly interested in forming such optically active nanodiamond centres to be used in quantum information systems for quantum cryptography or computing in connection with the Ni-N and N-V defect centres[19].

References

[1] F. Aumayr and H. Winter, e-J. Surf. Sci. Nanotech. Vol. 1 (2003) 171-174

[2] J.D. Gillaspy, J. Phys. B: At. Mol. Opt. Phys. 34 (2001) R93–R130

[3] A. Arnau, F. Aumayr, P.M. Echenique, M. Grether, W. Heiland, J. Limburg, R. Morgenstern, P. Roncin, S.Schippers, R. Schuch, N. Stolterfoht, P. Varga, T.J.M. Zouros and HP. Winter, Surf. Sci. Rep. 27, (1997) 113

[4] T. Schenkel, A. V. Hamza, A. V. Barnes, and D. H. Schneider, Prog. Surf. Sci. 61, (1999) 23

[5] T. Schenkel, A.V. Hamza, A.V. Barnes, D.H. Schneider, Progress in Surface Science 61 (1999) 23-84.

[6] T. Schenkel, A.V. Barnes, M.A. Briere, A.V. Hamza, A. Schach von Wittenau, D.H. Schneider, Nucl. Inst. Meth. Phys. Res. B 125 (1997) 153

[7] I.S. Bitensky, E. Parilis, S. Della-Negra, Y. Le Beyee, Nucl. Inst. Meth. Phys. Res. B 72 (1992) 380.

[8] Hai-Ping Cheng and J. D. Gillaspy, Phys. Rev. Vol. 55, No 4 (1997) 2628-2635

[9] T Schenkel, M. Schneider, M. Hattass, M. W. Newman, A. V. Barnes, A. V. Hamza, D.H. Schneider, R. L. Cicero, C. E. D. Chidsey, J. Vac. Sci. Technol. B 16, (1998) 3298

[10] C. Rühlicke, M. A. Briere, and D. H. Schneider, Nucl. Instr. Meth. B 99, (1995) 528 [11] R. Minniti, L.P. Ratliff and J. D. Gillaspy, Physica Scripta T92 (2001) 22-26

[12] I.C. Gebeshuber, S. Cernusca, F. Aumayr, H.P. Winter, International Journal of Mass Spectrometry 229 (2003) 27–34

[13] C. Lemell et al., Sol. St. El. 51, (2007) 1398

[14] A.V. Hamza, M.W. Newman, P.A. Thielen, H.W.H. Lee, T. Schenkel, J.W. McDonald, D.H. Schneider, Appl. Phys. A 76 (2003) 313.

[15] T. Meguro, A. Hida, M. Suzuki, Y. Koguchi, H. Takai, Y. Yamamoto, K. Maeda, Y. Aoyagi, Appl. Phys. Lett. 79 (2001) 3866.

[13] A. Hida, T. Meguro, K. Maeda, Y. Aoyagi, Nucl. Instr. and Meth. B 205 (2003) 736.

[16] T. Meguro, A. Hida, Y. Koguchi, S. Miyamoto, Y. Yamamoto, H. Takai, K. Maeda, Y. Aoyagi, Nucl. Instr. and Meth. B 209 (2003) 170.

[17] I.C. Gebeshuber, S. Cernusca, F. Aumayr, H.P. Winter, International Journal of Mass Spectrometry 229 (2003) 27–34

[18] R. Minniti, L.P. Ratliff and J. D. Gillaspy, Physica Scripta T92 (2001) 22-26 [19] Masahide Tona a, Yukari Baba b, Satoshi Takahashi b, Kazuo Nagata b,Nobuyuki Nakamura b, Nobuo Yoshiyasu c, Chikashi Yamada c, Shunsuke Ohtani b., Nuclear Instruments and Methods in Physics Research B 235 (2005) 443–447.

[20] C. D. Weis, et al., arXiv:0806.2167, J. Vac. Sci. Technol. B, in press

[21] F. Jelezko, T. Gaebel, I. Popa, M. Domhan, A. Gruber, J. Wrachtrup, Phys. Rev. Lett. 93, (2004) 130501 [22] [T. Schenkel et al., Rev. Sci. Instr. 73, (2002) 663

[23] M. Tona, Y. Baba, S. Takahashi , K. Nagata, N. Nakamura, N Yoshiyasu, C. Yamada, S. Ohtani b, Nuclear Instruments and Methods in Physics Research B 235 (2005) 443–447

[24] Yukari Baba a,1, Kazuo Nagata a, Satoshi Takahashi a, Nobuyuki Nakamura a, Nobuo Yoshiyasu a, Makoto Sakurai b,

Chikashi Yamada a, Shunsuke Ohtani a,c, Masahide Tona a,c, Surface Science 599 (2005) 248–254

[25] T. Meguro a,Y. Yamaguchi b, H. Fukagawa b, H. Takai b, N. Hanano c, Y. Yamamoto c, K. Kobashi d, T. Ishii d, Nuclear Instruments and Methods in Physics Research B 235 (2005) 431–437.

[26] Т. Schenkel,A. Persaud, S. J. Park, and J. Meijer, J. R. Kingsley, J. W. McDonald and J. P. Holder, J. Bokor, D. H. Schneider, J. Vac. Sci. Technol. B 20.6., Nov-Dec 2002.